applied sciences

MDPI

Article

Monte Carlo Investigation of Gamma Radiation Shielding Features for Bi_2O_3/Epoxy Composites

Karem G. Mahmoud [1,*], M. I. Sayyed [2,3], Aljawhara H. Almuqrin [4], Jack Arayro [5] and Yasser Maghrbi [6]

1 Department of Nuclear Power Plants and Renewable Energy, Ural Energy Institute, Ural Federal University, 19 Mira Street, 620002 Yekaterinburg, Russia
2 Department of Physics, Faculty of Science, Isra University, Amman 11622, Jordan
3 Department of Nuclear Medicine Research, Institute for Research and Medical Consultations (IRMC), Imam Abdulrahman bin Faisal University (IAU), P.O. Box 1982, Dammam 31441, Saudi Arabia
4 Department of Physics, College of Science, Princess Nourah bint Abdulrahman University, P.O. Box 84428, Riyadh 11671, Saudi Arabia
5 College of Engineering and Technology, American University of the Middle East, Eqaila 54200, Kuwait
6 University of Tunis El Manar, Tunis 2092, Tunisia
* Correspondence: karemabdelazeem@yahoo.com

Abstract: Three different samples were synthesized based on polyepoxide resin, a solidifying agent, and a Bi_2O_3 doping compound. The polyepoxide resin and solidifying agent were added in a 2:1 ratio by weight and the Bi_2O_3 compound was added in ratios of 0, 5, and 10 wt. %. The density of the synthesized composites was measured using an MH-300A densimeter with an uncertainty in measurement of 0.001 g/cm^3. The measurements showed that the density of the fabricated composite varied from 1.103 g/cm^3 to 1.20 g/cm^3 when the reinforcing Bi_2O_3 compound was raised from 0 wt. % to 10 wt. %. Furthermore, the γ-ray shielding parameters were evaluated based on the simulated mean track length of γ-photons inside the synthesized composites using MCNP-5 code. The simulated results show an enhancement in the shielding parameter when increasing the Bi_2O_3 concentration, where the linear attenuation coefficient values increased from 0.101 cm^{-1} to 0.118 cm^{-1} as the Bi_2O_3 concentration increased from 0 to 10 wt. %. The increase in the LAC has a positive effect on the other shielding properties.

Keywords: polyepoxide resin; Bi_2O_3 compound; Monte Carlo simulation; γ-ray properties

Citation: Mahmoud, K.G.; Sayyed, M.I.; Almuqrin, A.H.; Arayro, J.; Maghrbi, Y. Monte Carlo Investigation of Gamma Radiation Shielding Features for Bi_2O_3/Epoxy Composites. *Appl. Sci.* **2023**, *13*, 1757. https://doi.org/10.3390/app13031757

Academic Editor: José A. Jiménez

Received: 6 January 2023
Revised: 19 January 2023
Accepted: 27 January 2023
Published: 30 January 2023

1. Introduction

In modern technological fields, radiation is of significant benefit in various applications. However, radiation can also be dangerous, and inappropriate exposure to ionizing radiation caan bring extra health concerns. Lead (Pb) has been utilized as a photon absorber in a variety of applications, including personalized radiation protection equipment, glass, walls, and so on. Despite these advantages, there has been a significant rise in worry about the drawbacks of lead, including its toxicity and weight. The former is due to the fact that lead is the cause of a multitude of health issues, in addition to having negative impacts on the environment when it is discarded [1–3]. A high atomic number, high thickness, and high density are the most important criteria that need to be satisfied by a material before it can be used as a radiation attenuator [4–7], and high-quality lead-free materials should be lightweight and flexible in addition to being eco-friendly. The aim is to develop materials that are more comfortable than those that have historically used lead, and which in turn meet the requirements of the ALARA concept. In contrast to conventional materials, polymer composites, which have preferred qualities, are a modern technique for developing unique applications [8–10]. Polymers have been employed in several applications due to their interesting features. These applications include construction, aerospace, optical devices, radiation protection, biomedicine, automotive, and more. Furthermore,

polymers have found widespread application in the medical industry as a result of their biocompatibility, their resistance to heat and chemicals, and the ease with which they may be manufactured. As a result, polymers are an appealing choice for the development of innovative radiation protection materials because they are inexpensive, chemically stable, lightweight, and possess excellent mechanical features. In addition, polymers are able to considerably reduce the effects of ionizing radiation by utilizing metal structures with both high atomic weights and densities as composites [11–13].

Epoxy resin is a form of reactive prepolymer and a polymer that contains epoxide groups in both its monomer and its polymer chains. These resins can either react with one another in the presence of catalysts or with a large number of other co-reactants. Epoxy resin is extensively used in the industrial sector for a wide range of projects. For example, on one hand, epoxy is the most common type of resin utilized in the electronic industry for overmolding integrated circuits, hybrid circuits, and transistors. On the other hand, the fabrication of advanced radiation shielding materials may be achieved in an efficient manner by incorporating heavy metal oxides, such as Bi_2O_3, into the epoxy matrix [14–17]. As a result of the wide variety of uses that may be found for heavy metal oxides, there has been a lot of interest in these compounds in both the academic and commercial sectors. The most obvious feature of Bi_2O_3 is its high density, and thus a relatively high-density polymer composite is expected when high concentrations of Bi_2O_3 are used. In addition, bismuth (Bi), which is currently under investigation as a possible candidate material for lead (Pb) replacement in radiation protection, is starting to play a useful role in the creation of next-generation shielding components with much more favorable characteristics [18–20]. In view of the significance of incorporating Bi_2O_3 into epoxy resin as a filler, the primary emphasis of this research was on the radiation-shielding applications of epoxy matrices, which are inexpensive and simple to manufacture. In order to provide a theoretical and simulation-based contribution to the ongoing research on radiation protection using epoxy, Bi_2O_3 particles were introduced into epoxy resin in various mass fractions. Using Monte Carlo simulations, the radiation shielding capabilities of the prepared composites were calculated, and a comprehensive study was carried out by matching the findings of the simulation with the XCOM software results.

2. Materials and Methods

Three samples were synthesized at room temperature based on polyepoxide resin, a solidifying agent, and a reinforcing Bi_2O_3 compound. The polyepoxides resin, as well as its solidifying agent, were bought from SlabDOC (Ivanovo, Russia) at a purity of 98%. The polyepoxide resin was mixed with the solidifying agent in a 2:1 ratio by weight for 10 min. After that, the required amount of Bi_2O_3 was weighed using a sensitive electric balance and added to the mixture with continued stirring for another 15 min. Then, the mixture was cast in a cylindrical mold and allowed to solidify for 24 h. The final products of the synthesized composites are presented in Figure 1. A MXBAOHENG MH 300A (Guangdong, China) density meter was used to measure the density of the synthesized composites with an uncertainty of 0.01 g/cm^3. The measurements show that the densities of the polyepoxide-reinforced Bi_2O_3 composites were 1.103, 1.159, and 1.20 g/cm^3. The composition of the fabricated composites was then determined using X-ray fluorescence (XRF) (see Table 1).

Table 1. Elemental composition and density of the synthesized composites.

	Elemental Composition (wt.%)		
	Bi_2O_3 0%	**Bi_2O_3 5%**	**Bi_2O_3 10%**
H	6.97	6.61	6.26
C	44.01	41.77	39.54
O	36.32	35.00	33.68

Table 1. *Cont.*

	Elemental Composition (wt.%)		
	Bi_2O_3 0%	**Bi_2O_3 5%**	**Bi_2O_3 10%**
Na	2.34	2.22	2.10
Cl	8.48	8.05	7.62
K	1.49	1.42	1.34
Co	0.17	0.16	0.15
Bi	0.00	4.55	9.10
Density (g/cm^3)	1.103 ± 0.033	1.159 ± 0.034	1.200 ± 0.036

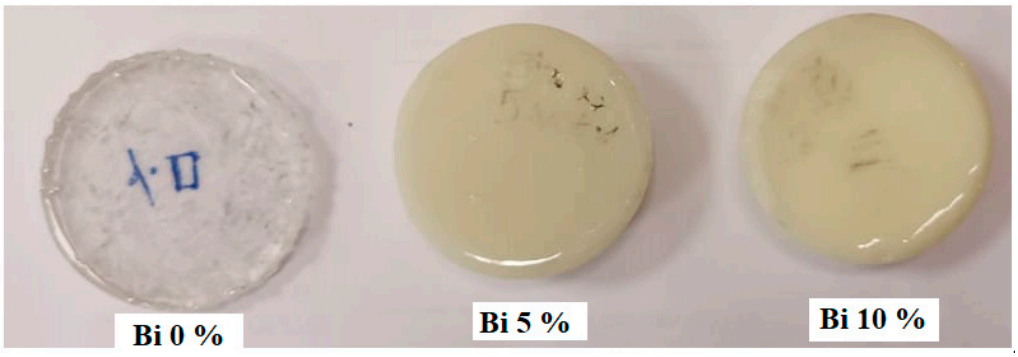

Figure 1. Fabricated polyepoxide-reinforced Bi_2O_3 composites.

The elemental chemical composition obtained by the X-ray fluorescence and the density recorded by the MH 300A densimeter were utilized to estimate the γ-ray shielding properties of the samples utilizing MCNP-5 [21]. The simulation was done over a wide gamma energy (E_γ, keV) interval, which varied between 15 keV and 661 keV. The geometry used in the present work has been described elsewhere [22–24]. A radioactive source was placed at the origin of the geometry (at 0 0 0), emitting photons along the Z-direction. The photon energies, emission probability, and the photon distribution were introduced to the source card (SDEF). The radioactive source was surrounded by a lead collimator with a 1 cm slit to direct the photon flux to the fabricated samples. The sample was placed at a distance of 7 cm from the radioactive source and 5 cm from the detector. The Bi_2O_3-doped polyepoxide resin composites had a diameter of 3 cm and various thicknesses. The photons transmitted from the fabricated composite were collimated using a second collimator and directed to the detector. The tally used in the present work to calculate the average photon flux per unit cell of the fabricated composite was F4. The average photon flux was utilized to estimate the mean track length (MTL) of γ-photons inside the fabricated composites. The simulation was carried out and a new output MCNP-5 file, in the form of a txt file, was created, containing all the information about the mean track length of γ-photons inside the fabricated composites at the selected γ-ray energy interval. The relative error in the simulated data, according to the output file, was in the range of ±1%. The obtained MTL of γ-photons was converted to shielding parameters through the following equations:

$$\mu\left(cm^{-1}\right) = \frac{I}{x}\ln\left(\frac{I_o}{I_t}\right) \quad (1)$$

The half-value thickness ($\Delta_{0.5}$, cm) is defined as:

$$\Delta_{0.5}\ (cm) = \frac{\ln(2)}{\mu} \quad (2)$$

$$TF\ (\%) = \frac{I_t}{I_o} \times 100 \quad (3)$$

$$\text{RPE}\ (\%) = \frac{I_a}{I_o} \times 100 \quad (4)$$

I_a refers to the absorbed photon number inside the synthesized composites.

3. Results and Discussion

The μ for the fabricated polyepoxide-reinforced Bi_2O_3 composites was evaluated via determination of the MTL of the emitted γ-photons using MCNP-5 code in the γ-photon energy (E_γ, keV) interval between 15 and 661 keV, as illustrated in Figure 2. The studied E_γ interval contains two different γ-photon interaction modes. The first is the photoelectric interaction (PE) which extends along the interval from 15 to 122 keV, where the μ values suffer from a high reduction with increasing E_γ values. This high reduction in the μ value can be attributed to the PE cross-section, which varied inversely with $E^{3.5}$. The μ values decreased in the mentioned interval by factors of 95.0, 96.3, and 96.6% for the fabricated composites Bi_2O_3 0%, Bi_2O_3 5%, and Bi_2O_3 10%, respectively, when the E_γ increased from 15 to 122 keV. The second mode of γ-photon interaction in the current work is Compton scattering (CS), which extended from 200 keV to 661 keV. In the second mentioned interval, the μ values decreased moderately under the effect of CS cross-section when the E_γ value increased, where the CS cross-section was inversely correlated with E. For example, the μ values decreased by factors of 27.7, 34.2, and 39.6%, for composites Bi_2O_3 0%, Bi_2O_3 5%, and Bi_2O_3 10%, respectively, when E_γ increased from 200 to 661 keV.

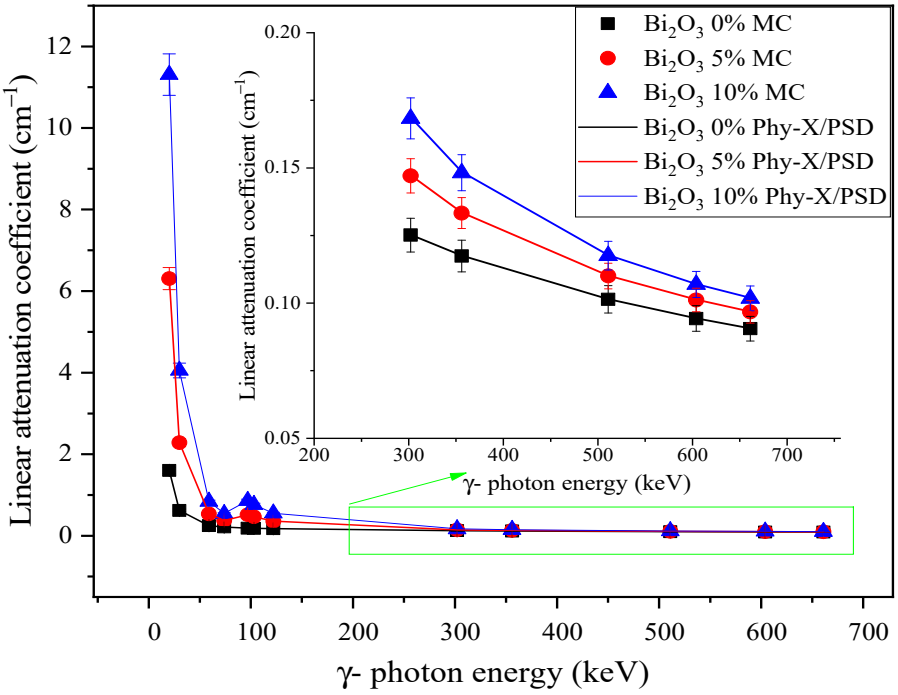

Figure 2. The linear attenuation coefficient of the polyepoxide-reinforced Bi_2O_3 composites.

The impact of the Bi_2O_3 doping content on the μ of the fabricated composites is illustrated in Figure 3. The results presented in the figure show that the μ increased significantly with rising Bi_2O_3 ratios. In the PE interaction mode, the μ values recorded a large increase with rising Bi_2O_3 concentration. This large increase is attributed to the PE cross-section, which varies directly with Z_{eff}^{4-5}, where Z_{eff} refers to the effective atomic number. In the aforementioned E_γ interval, the μ values increased by factors of 362, 236, and 218% at E_γ values of 15 keV, 59 keV, and 122 keV, respectively, when the Bi_2O_3 doping concentration increased from 0 to 10 wt.%. The obtained results show that, in the CS interaction region, the μ values increased slightly with rising Bi_2O_3 concentration. For instance, at an E_γ of 661 keV, the μ values increased by 12% by raising the Bi_2O_3 doping concentration from 0 to 10 wt.%.

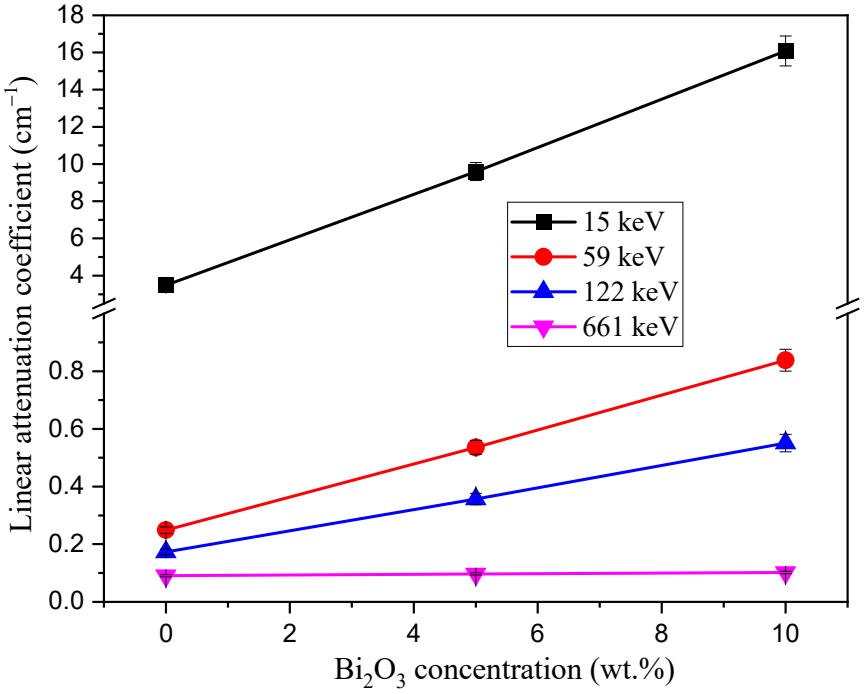

Figure 3. Influence of Bi_2O_3 concentration on the LAC of the synthesized composite.

The mass attenuation coefficient (μ_m) for the polyepoxide-reinforced Bi_2O_3 composites was calculated, first based on the simulated results, then using the free program Phy-X/PSD [25]. Moreover, the μ_m for the selected composites was determined experimentally via the narrow beam transmission method using the γ-photons emitted from radioactive sources Am-241, Na-22, and Cs-137 with energies of 59, 511, and 661 keV, respectively. The measurements for the unattenuated photons (I_o) and the attenuated photons (I) were detected using a 3″ × 3″ NaI (Tl) detector. Table 2 shows a comparison between the simulated, theoretically calculated (Phy-X/PSD), and the experimental measurements. The comparison depicts a difference (δ, %) in the range of ±1% between MCNP and Phy-X data, whereas the difference between the experimental measurement and the MCNP simulation was found to be approximately ±6%.

The thickness of polyepoxide-reinforced Bi_2O_3 composites required to reduce the emitted photons by a factor of 50% is called the half-value thickness ($\Delta_{0.5}$). Figure 4 depicts the variation in the $\Delta_{0.5}$ values versus E_γ. The $\Delta_{0.5}$ values increase with rising E_γ values due to the PE and CS interactions, as illustrated in the linear attenuation coefficient section. In the PE interaction interval (i.e., 15 keV < E_γ < 122 keV), the $\Delta_{0.5}$ rose from 0.20 to 4.01 cm (for Bi_2O_3 0%), from 0.07 to 1.94 cm (for Bi_2O_3 5%), and from 0.04 to 1.26 cm (for Bi_2O_3 10%). This rapid increase in $\Delta_{0.5}$ values is attributed to the large decrease in the μ values under the effect of the PE interaction. The results in Figure 4 also show that the $\Delta_{0.5}$ values linearly increase when E_γ values increase from 302 keV to 661 keV. For example, the increase in $\Delta_{0.5}$ values from 5.54 to 7.66 cm (for Bi_2O_3 0%), from 4.71 to 7.17 (for Bi_2O_3 5%), and from 4.12 to 6.81 cm (for Bi_2O_3 10%) is accompanied by an increase in E_γ from 302 keV to 661 keV. This moderate increase in the $\Delta_{0.5}$ values is attributed to the CS cross-section, in which the μ values of the fabricated composites decrease exponentially with rising E_γ values.

We calculated the relaxation length (λ, cm), which is inversely proportional to μ ($\lambda = 1/\mu$). The calculated values for λ show the same trend in variation with E_γ as the $\Delta_{0.5}$ values. In contrast, the λ values increased from 0.29 to 11.05 cm (for Bi_2O_3 0%), from 0.10 to 10.34 cm (for Bi_2O_3 5%), and from 0.06 to 9.83 cm (for Bi_2O_3 10%), by raising the E_γ values from 15 to 661 keV.

Table 2. The mass attenuation coefficient simulated by MCNP-5 code XCOM online software.

Energy/keV	μ_m (cm^2/g)								
	Bi_2O_3 0%			Bi_2O_3 5%			Bi_2O_3 10%		
	MCNP	Phy-X/PSD	EXP	MCNP	Phy-X/PSD	EXP	MCNP	Phy-X/PSD	EXP
15	3.155	3.152		8.278	8.282		13.396	13.400	
20	1.452	1.451		5.442	5.458		9.426	9.459	
30	0.565	0.564		1.972	1.973		3.378	3.379	
59	0.226	0.226	0.236	0.462	0.464	0.486	0.698	0.702	0.729
74	0.194	0.195		0.323	0.325		0.451	0.456	
97	0.171	0.171		0.443	0.446		0.715	0.719	
103	0.167	0.167		0.401	0.402		0.635	0.636	
122	0.157	0.157		0.308	0.308		0.459	0.459	
302	0.113	0.114		0.127	0.127		0.140	0.141	
356	0.106	0.107		0.115	0.115		0.124	0.124	
511	0.092	0.092	0.096	0.095	0.095	0.099	0.098	0.098	0.103
604	0.085	0.086		0.087	0.087		0.089	0.089	-
661	0.082	0.082	0.085	0.083	0.084	0.087	0.085	0.085	0.089

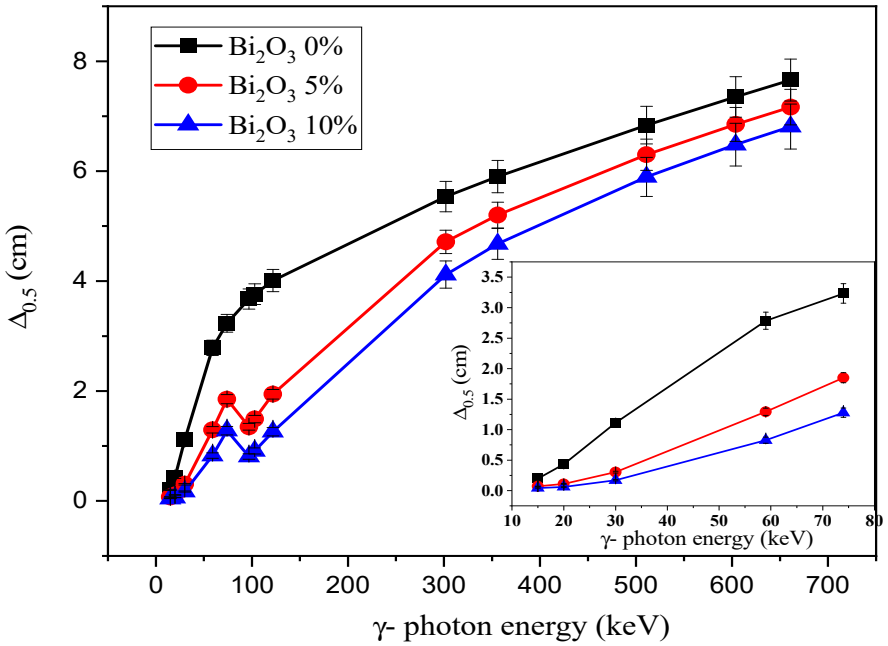

Figure 4. Variation in the half-value thickness of the polyepoxide-reinforced Bi_2O_3 composites versus the γ-photon energy.

The $\Delta_{0.5}$ and λ values were strongly affected by the Bi_2O_3 doping concentration, as illustrated in Figure 5. The obtained results show that the $\Delta_{0.5}$ and λ decreased by approximately 75% with an increase in the Bi_2O_3 doping ratio in the PE interval, whereas they decreased by approximately 16% in the CS interval when the Bi_2O_3 concentration increased between 0 and 10 wt. %. For example, at an E_γ value of 551 keV, the $\Delta_{0.5}$ values decreased from 6.84 to 5.90 cm, whereas the λ values decreased from 9.86 to 8.51 cm as the Bi_2O_3 concentration increased from 0 to 10 wt. %. This decrease in the $\Delta_{0.5}$ and λ values with the addition of Bi_2O_3 is attributed to the increase in the interaction cross-section with increasing Z_{eff} of the fabricated composites.

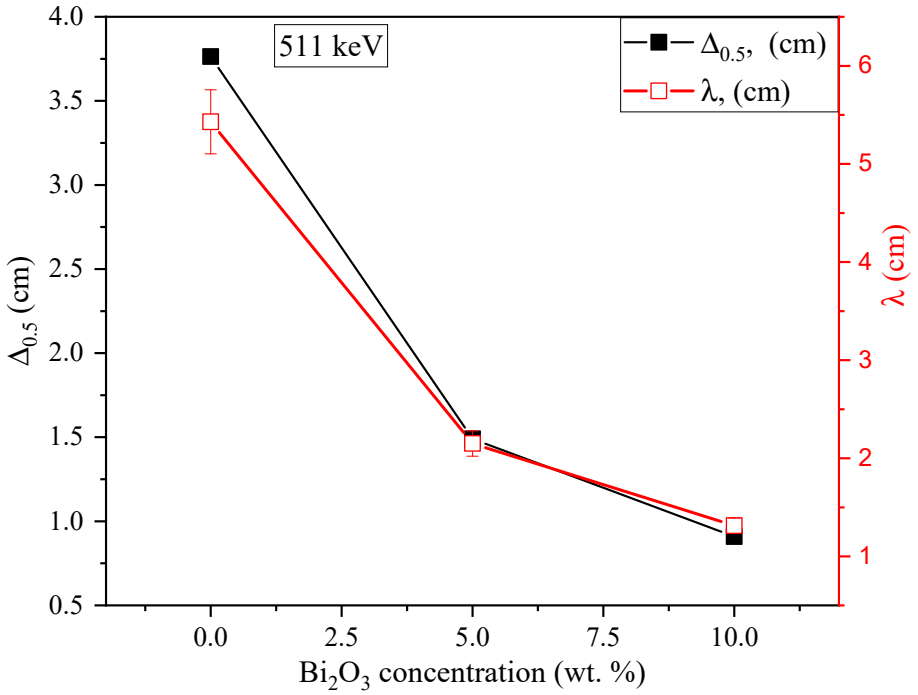

Figure 5. Influence of Bi_2O_3 concentration on $\Delta_{0.5}$ and relaxation length (λ, cm).

The efficiency of the material can be also estimated through comparison of the number of transmitted photons (I_t) with the total number of emitted photons (I_o), where the transmission factor, TF, (%) = (I_t/I_o) × 100. In this study, the TF and RPE values were mainly affected by three parameters: emitted photon E_γ, Bi_2O_3 doping concentration, and fabricated composite thickness. Increasing the emitted photon energy, E_γ, caused a large increase in the penetration power of the emitted photons, which affects the values of I_t and I_a. We found that a large increase in the number of I_t photons was accompanied by a decrease in the number of I_a photons. So, the TF increase is accompanied by a decrease in the RPE, leading to an increase in E_γ values. For example, a 1 cm thickness of the fabricated Bi_2O_3 10% sample had TF values that varied between 0 and 90 wt. %, whereas it had RPE values that decreased from 100 to around 9%, when the E_γ increased from 15 to 661 keV.

The Bi_2O_3 concentration also affects TF and RPE. Figure 6 shows the TF and RPE versus the Bi_2O_3 doping concentration. Raising the Bi_2O_3 content in the composites increases the composites' Z_{eff}, which causes an increase in the resistance of the composite towards the passage of the emitted photons. Thus, the increase in photon–electron interactions inside the fabricated material is associated with a decrease in I_t photons and a significant increase in I_a photons. As a result, when TF decreases there is an associated increase in the RPE values. For example, at an E_γ of 122 keV, TF values decreased from 84.1% to 57.7% and RPE values rose from 15.9% to 42.3% as the Bi_2O_3 concentration increased from 0 to 10 wt. %. Moreover, it has been found that the composite's thickness also affects TF and RPE, as illustrated in Figure 7. For example, at an E_γ of 122 keV, the TF values of the fabricated Bi_2O_3 10% composite decreased from 65.8% to 1.5%, whereas RPE values increased from 34.2% to 98.5% as the composite thickness increased from 0.5 to 5 cm. Raising the fabricated composite thickness from 0.5 to 5 cm caused an bigger increase in the path length of the photons than the relaxation length of photons. Thus, the emitted photon performs more collisions inside the fabricated composite before penetrating the composite bulk. As a result, there is an increase in I_a and a significant decrease in the number of I_t photons. Therefore, the decrease in TF is associated with an increase in RPE values.

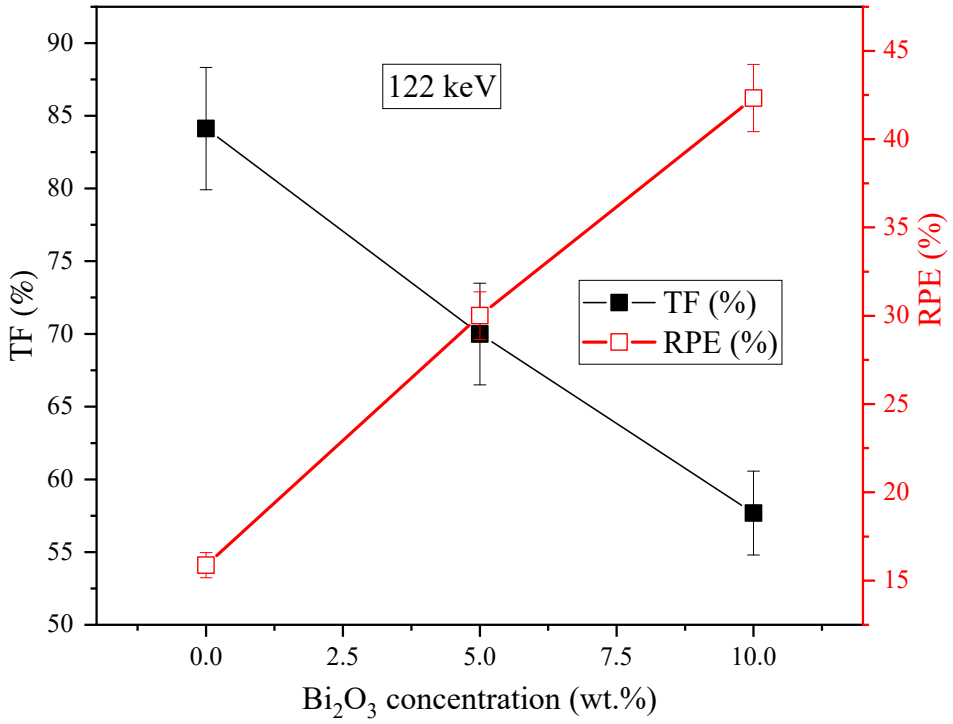

Figure 6. Dependence of transmission factor (TF, %) and RPE on the Bi_2O_3 concentrations at a γ-photon energy of 122 keV.

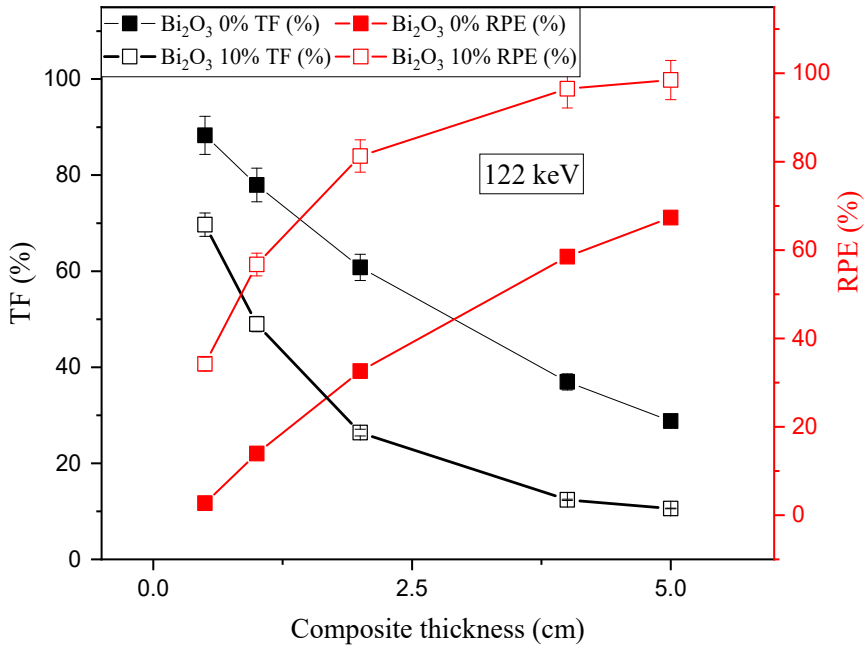

Figure 7. Dependence of TF and RPE on the composite thickness for composites Bi 0% and Bi 10%.

The Z_{eff} is the parameter used to examine the attenuation properties of a multi-element composite in terms of its equivalent element. Figure 8 depicts the Z_{eff} for the current samples versus the γ-photon energy. For example, at an E_γ of 15 keV, the fabricated composites, Bi_2O_3 0%, Bi_2O_3 5%, and Bi_2O_3 10%, have shielding parameters similar to Na (Z = 11), Cr (Z = 24), and Se (Z = 34), respectively. These values for Z_{eff} decrease when the emitted gamma photon energy increases. For example, at E_γ values between 15 keV and 661 keV, the fabricated composites, Bi_2O_3 0%, Bi_2O_3 5%, and Bi_2O_3 10%, act as Be (Z = 4), B (Z = 5), and C (Z = 6), respectively. Figure 8 shows two peaks where the Z_{eff}

has an unexpected increase. This increase in the Z_{eff} values is attributed to the L1 and K absorption edges of Bi that appear at 16.3 keV and 90.5 keV, respectively.

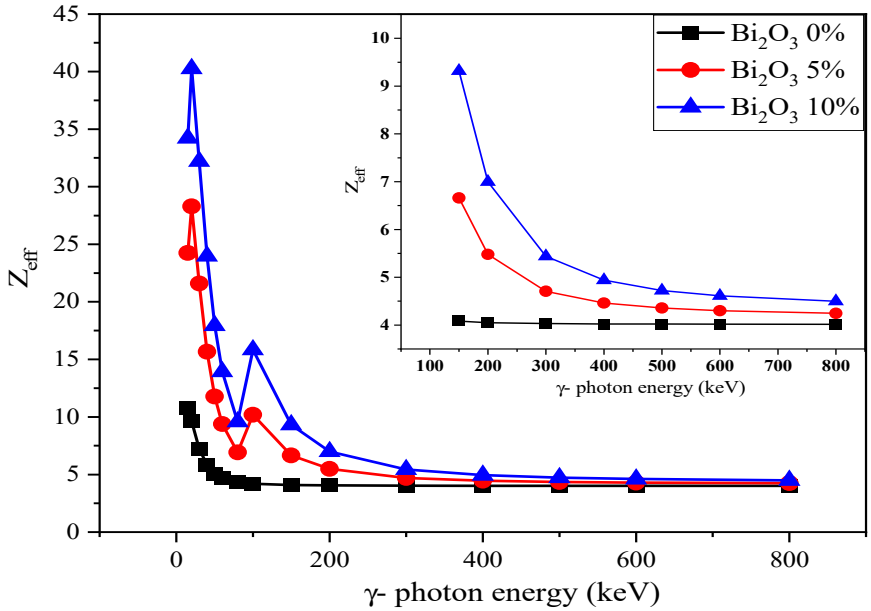

Figure 8. Variation in the effective atomic number (Z_{eff}) of the synthesized polyepoxide-reinforced Bi_2O_3 composites versus the emitted γ-photon energy.

Buildup factors are also key to clarifying the ability of a material to get rid of the emitted photons and to prevent their accumulation in the material bulk. The buildup factor is divided into two parts: the exposure buildup factor (EBF) and the energy absorption buildup factor (EABF). In order to calculate both the EBF and EABF, it is necessary to first determine the value of the equivalent atomic number (Z_{eq}), which describes a multielement material in terms of its equivalent element. However, unlike Z_{eff}, Z_{eq} depends on the ratio of the Compton scattering mass, μ_m, to the total μ_m. Calculations of Z_{eff}, Z_{eq}, EBF, and EABF were performed using Phy-X/PSD software [25]. Figure 9 shows that the values of Z_{eq} were very small at low E_γ energies. This decrease in the Z_{eq} is related to the reduced values of (μ_m) Compton scattering due to the predominance of the PE interaction. In the PE interaction region, Z_{eq} increases from 9.2 to 9.8 for Bi_2O_3 0%, from 12.4 to 26.4 for Bi_2O_3 5 %, and from 14.46 to 32.48 for Bi_2O_3 10 %. Above 100 keV, the Z_{eq} values were greatly increased due to the predominance of CS interactions, and the (μ_m) Compton scattering was greatly increased compared to the total μm values.

EBF and EABF values were calculated and are presented in Figures 10 and 11 along with the γ-photon energy and Bi_2O_3 doping concentration. The values of these factors were very low at low E_γ values, they then increase gradually with rising E_γ in the CS region. For the Bi 0% composite, without Bi_2O_3, the EBF and EABF tend to reach maximum values at around 150 keV, where the EBF and EABF values were 117 and 164, respectively. Then, both EBF and EABF reduce gradually and drop to 29.2 and 32.6 under the effect of pair production (PP), which consumes the photon energy in the production of an electron and positron pair. Raising the Bi_2O_3 concentration in the fabricated composites causes a high decrease in the EBF and EABF; the EBF values at 15 keV decreased from 1.09 to 1.06, whereas the EABF values decreased from 1.09 to 1.05. The results show that the addition of Bi_2O_3 to the polyepoxide resin reduces the accumulation of photons in the fabricated composite. This observation can be attributed to the Z_{eff} of the composites, where increasing the Bi_2O_3 composition causes an increase in the fabricated composite's Z_{eff}. Hence, the PE interaction cross-section is directly proportional to Z^{4-5}. Consequently, the probability of this process increases with the increasing Z_{eff}. Thus, the energy of the emitted photon is totally consumed in the interaction with the composite atoms and electrons. So, the

EBF and EABF values show a significant decrease with rising Bi_2O_3 concentration in the fabricated composites.

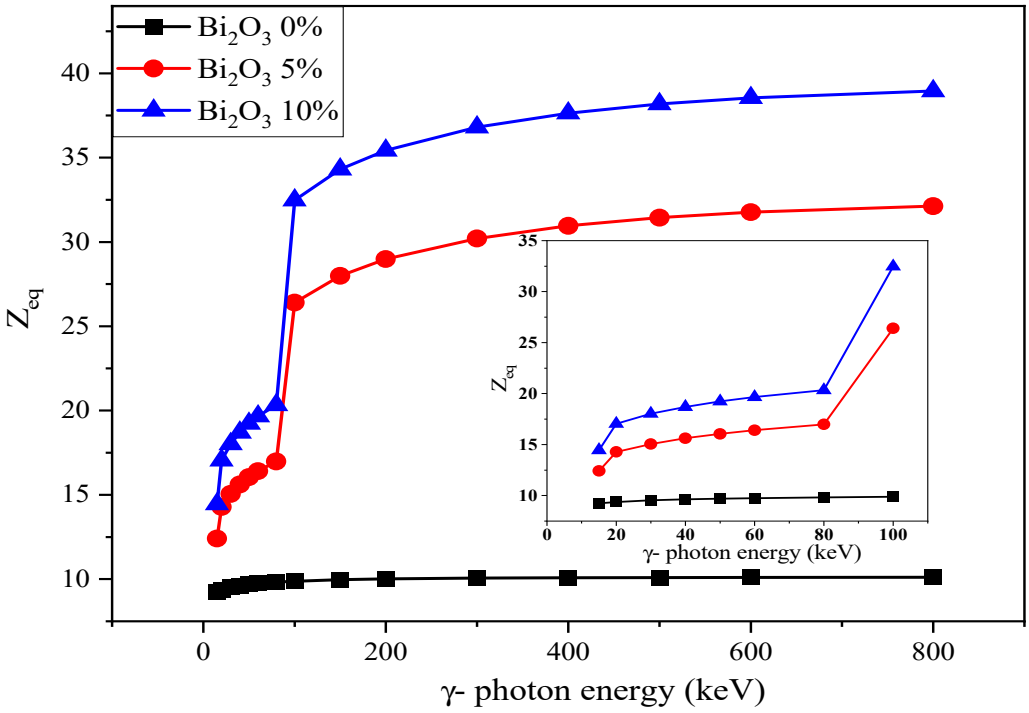

Figure 9. Variation in the equivalent atomic number (Z_{eq}) of the fabricated polyepoxide-reinforced Bi_2O_3 composites versus the emitted γ-photon energy.

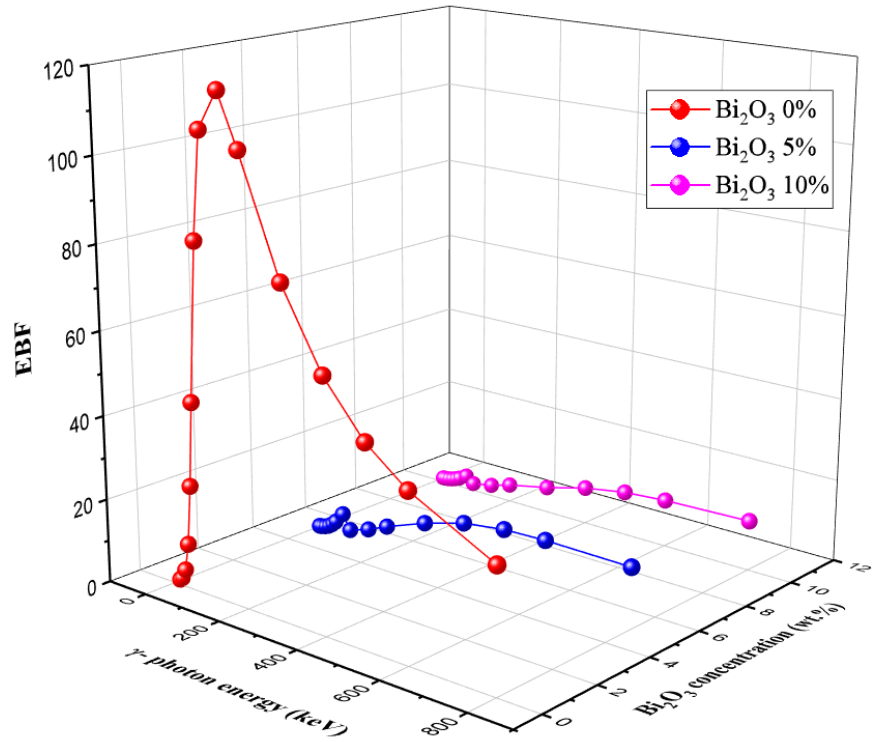

Figure 10. Variation in the EBF of the fabricated polyepoxide-reinforced Bi_2O_3 composites versus the emitted γ-photon energy and Bi_2O_3 concentration at 10 mfp.

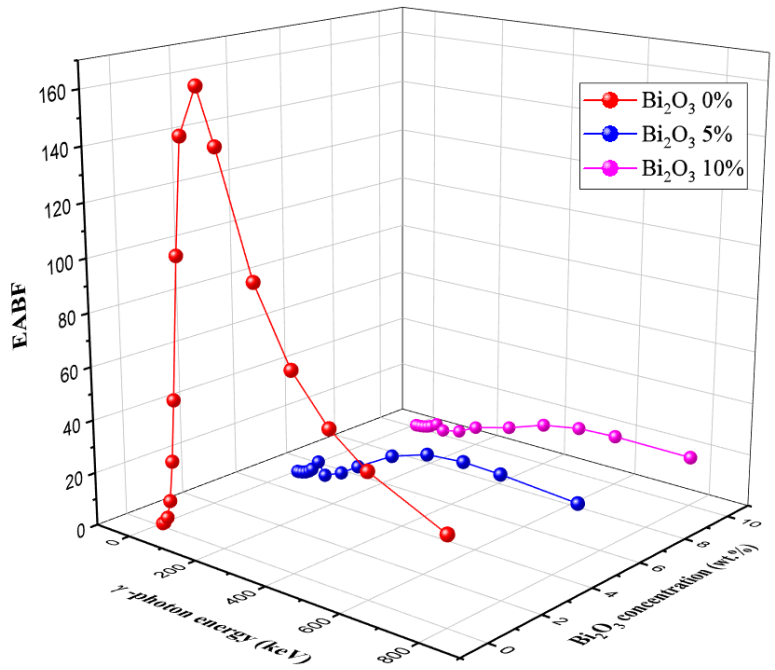

Figure 11. Variation in the EBF of the fabricated polyepoxide-reinforced Bi_2O_3 composites versus the emitted γ-photon energy and Bi_2O_3 concentration.

Moreover, raising the penetration depth in the unit of a mean free path (mfp) causes an increase in both EBF and EABF for the fabricated composites. Figure 12 shows that the increase in the EBF and EABF values is low at small values of penetration depth, whereas the EBF and EABF increase greatly at high values of penetration depth (especially for penetration depths higher than 20 mfp). Increasing the penetration depth forces the incident photons to stay for longer inside the fabricated samples and perform many collisions with the surrounding electrons. Therefore, the number of photons accumulated inside the material increases with increasing penetration depth. Another observation from Figure 12 is that raising the Bi_2O_3 concentration in the fabricated composites reduces the number of accumulated photons inside the material. This is ascribed to the increase in the probability of PE interaction with increasing Bi_2O_3 concentration at the studied energy of 60 keV. Thus, the photon's energy is consumed totally during the interaction (the energy is consumed to eject one of the boundary electrons from the atoms). Thus, the increase in Bi_2O_3 concentration is accompanied by a significant reduction in the EBF and EABF values at low energy intervals.

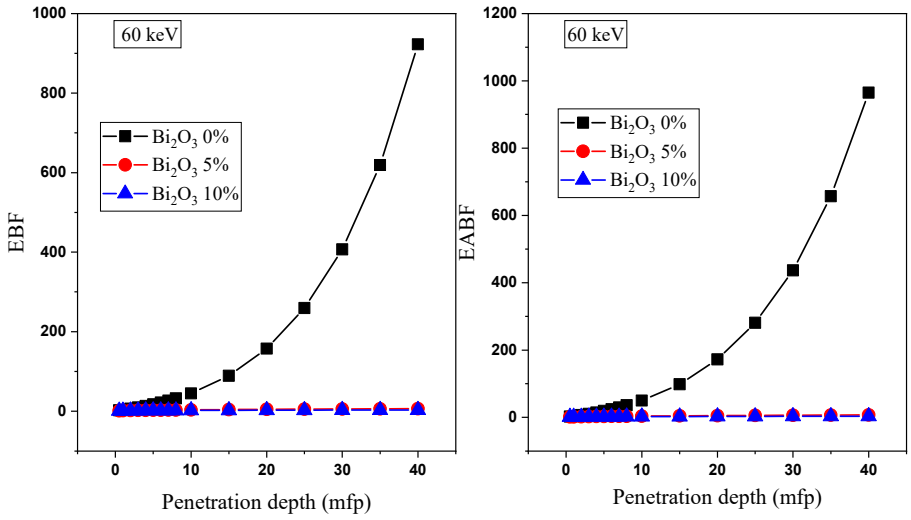

Figure 12. Variation in EBF and EABF values versus the penetration depth.

4. Conclusions

A series of epoxy-reinforced Bi_2O_3 compounds were synthesized using polyepoxide resin and a solidifying agent at room temperature. The density of the synthesized composites was enhanced from 1.103 to 1.20 g/cm^3 by raising the concentration of Bi_2O_3 composite from 0 wt.% to 10 wt.%. The ability of the synthesized composites to attenuate the low γ-photon energies was estimated using the Monte Carlo simulation N-Particle transport code in the E_γ interval between 15 keV and 661 keV. The estimated results show that the μ values are enhanced by raising the Bi_2O_3 concentration in the synthesized composites. For example, at an E_γ of 661 keV, the μ values are enhanced by a factor of 12.4%, where the μ values increased from 0.091 cm^{-1} to 0.102 cm^{-1} as the Bi_2O_3 concentration increased from 0 to 10 wt. %. The aforementioned enhancement in the μ values was also reflected in the other shielding properties, where the half-value thickness and mean free path decreased with rising Bi_2O_3 concentration. Moreover, the TF values decreased and the associated RPE increased with rising Bi_2O_3 concentration in the synthesized composites. Furthermore, the Phy-X/PSD results for buildup factors show a decrease in their values with increasing Bi_2O_3 concentration.

Author Contributions: K.G.M.: Conceptualization; Methodology; Software; Writing—original draft, Writing—review & editing; M.I.S. Conceptualization; Methodology; Investigation; Writing—original draft, Writing—review & editing; A.H.A.: Funding acquisition; Sueprvision; J.A.: Writing—review & editing, Funding acquisition; Y.M.: Writing—review & editing, Funding acquisition. All authors have read and agreed to the published version of the manuscript.

Funding: The authors express their gratitude to Princess Nourah bint Abdulrahman University researchers supporting Project number (PNURSP2023R2), Princess Nourah bint Abdulrahman University, Riyadh, Saudi Arabia.

Institutional Review Board Statement: Not applicable.

Informed Consent Statement: Not applicable.

Data Availability Statement: All relevant data are within this paper.

Conflicts of Interest: The authors declare no conflict of interest.

References

1. Nunez-Briones, A.G.; Benavides, R.; Bolaina-Lorenzo, E.D.; Martínez-Pardo, M.E.; Kotzian-Pereira-Benavides, C.; Mendoza-Mendoza, E.; Bentacourt-Galindo, R.; Garcia-Cerda, L.A. Nontoxic flexible PVC nanocomposites with Ta_2O_5 and Bi_2O_3 nanoparticles for shielding diagnostic X-rays. *Radiat. Phys. Chem.* **2023**, *202*, 110512. [CrossRef]
2. Intom, S.; Kalkornsurapranee, E.; Johns, J.; Kaewjaeng, S.; Kothan, S.; Hongtong, W.; Kaewkhao, J. Mechanical and radiation shielding properties of flexible material based on natural rubber/Bi_2O_3 composites. *Radiat. Phys. Chem* **2020**, *172*, 108772. [CrossRef]
3. Adliene, D.; Gilys, L.; Griskonis, E. Development and characterization of new tungsten and tantalum containing composites for radiation shielding in medicine. *Nucl. Instrum. Methods B* **2020**, *4671*, 21–26. [CrossRef]
4. Sayyed, M.I.; El-Mesady, I.A.; Abouhaswa, A.S.; Askin, A.; Rammah, Y.S. Comprehensive study on the structural, optical, physical and gamma photon shielding features of B_2O_3-Bi_2O_3-PbO-TiO_2 glasses using WinXCOM and Geant4 code. *J. Mol. Struct.* **2019**, *1197*, 656–665. [CrossRef]
5. Kaewjaeng, S.; Chanthima, N.; Thongdang, J.; Reungsri, S.; Kothan, S.; Kaewkhao, J. Synthesis and radiation properties of Li_2O-BaO-Bi_2O_3-P_2O_5 glasses. *Mater. Today Proc.* **2021**, *43*, 2544–2553. [CrossRef]
6. Kumar, A.; Gaikwad, D.K.; Obaid, S.S.; Tekin, H.O.; Agar, O.; Sayyed, M.I. Experimental studies and Monte Carlo simulations on gamma ray shielding competence of (30+x)PbO-10WO_3-10Na_2O−10MgO–(40-x)B_2O_3. *Prog. Nucl. Energy* **2020**, *119*, 103047. [CrossRef]
7. Kaewjaeng, S.; Kothan, S.; Chaiphaksa, W.; Chanthima, N.; Rajaramakrishna, R.; Kim, H.J.; Kaewkhao, J. High transparency La_2O_3-CaO-B_2O_3-SiO_2 glass for diagnosis x-rays shielding material application. *Radiat. Phys. Chem.* **2019**, *160*, 41–47. [CrossRef]
8. Azman, N.Z.N.; Siddiqui, S.A.; Low, I.M. Characterisation of micro-sized and nano-sized tungsten oxide-epoxy composites for radiation shielding of diagnostic X-rays. Mater. *Sci. Eng. C* **2013**, *33*, 4952–4957. [CrossRef]
9. Almuqrin, A.H.; Sayyed, M.I. Radiation shielding characterizations and investigation of TeO_2–WO_3–Bi_2O_3 and TeO_2–WO_3–PbO glasses. *Appl. Phys. A* **2021**, *127*, 190. [CrossRef]
10. Chang, L.; Zhang, Y.; Liu, Y.; Fang, J.; Luan, W.; Yang, X.; Zhang, W. Preparation and characterization of tungsten/epoxy composites for c-rays radiation shielding. *Nucl. Instrum. Methods Phys. Res. Sect. B* **2015**, *356–357*, 88–93. [CrossRef]

11. Li, R.; Gu, Y.; Zhang, G.; Yang, Z.; Li, M.; Zhang, Z. Radiation shielding property of structural polymer composite: Continuous basalt fiber reinforced epoxy matrix composite containing erbium oxide. *Compos. Sci. Technol.* **2017**, *143*, 67–74. [CrossRef]
12. Nagaraj, N.; Manjunatha, H.C.; Vidya, Y.S.; Seenappa, L.; Sridhar, K.N.; Damodara Gupta, P.S. Investigations on Lanthanide polymers for radiation shielding purpose. *Radiat. Phys. Chem.* **2022**, *199*, 110310. [CrossRef]
13. Vignesh, S.; Winowlin Jappes, J.T.; Nagaveena, S.; Krishna Sharma, R.; Adam Khan, M.; More, C.V. Preparation of novel in-situ layered B_4C and PbO reinforced solution casted layered polymer composites (SCLPC) for augmenting the gamma irradiation shielding capability. *Vacuum* **2023**, *207*, 111583. [CrossRef]
14. Aldhuhaibat, M.J.R.; Amana, M.S.; Jubier, N.J.; Salim, A.A. Improved gamma radiation shielding traits of epoxy composites: Evaluation of mass attenuation coefficient, effective atomic and electron number. *Radiat. Phys. Chem.* **2021**, *179*, 109183. [CrossRef]
15. Hashemi, S.A.; Mousavi, S.M.; Faghihi, R.; Arjmand, M.; Sina, S.; Aman, A.M. Lead oxide-decorated graphene oxide/epoxy composite towards X-Ray radiation shielding. *Radiat. Phys. Chem.* **2018**, *146*, 77–85. [CrossRef]
16. Canel, A.; Korkut, H.; Korkut, T. Improving neutron and gamma flexible shielding by adding medium-heavy metal powder to epoxy based composite materials. *Radiat. Phys. Chem.* **2019**, *158*, 13–16. [CrossRef]
17. Zali, V.S.; Jahanbakhsh, O.; Ahadzadeh, I. Preparation and evaluation of gamma shielding properties of silicon-based composites doped with WO_3 micro- and nanoparticles. *Radiat. Phys. Chem.* **2022**, *197*, 110150. [CrossRef]
18. Cao, D.; Yang, G.; Bourham, M.; Moneghan, D. Gamma radiation shielding properties of poly (methyl methacrylate)/Bi_2O_3 composites. *Nucl. Eng. Technol.* **2020**, *52*, 2613–2619. [CrossRef]
19. Karabul, Y.; İçelli, O. The assessment of usage of epoxy based micro and nano-structured composites enriched with Bi_2O_3 and WO_3 particles for radiation shielding. *Results Phys.* **2021**, *26*, 104423. [CrossRef]
20. Muthamma, M.V.; Prabhu, S.; Bubbly, S.G.; Gudennavar, S.B. Micro and nano Bi_2O_3 filled epoxy composites: Thermal, mechanical and γ-ray attenuation properties. *Appl. Radiat. Isot.* **2021**, *174*, 109780. [CrossRef]
21. X-5 Monte Carlo Team. *MCNP—A General Monte Carlo N-Particle Transport Code, Version 5*; La-Ur-03-1987. II; Los Alamos National Laboratory: Los Alamos, NM, USA, 2003.
22. Sayyed, M.I.; Zaid, M.H.M.; Effendy, N.; Matori, K.A.; Lacomme, E.; Mahmoud, K.A.; AlShammari, M.M. The influence of PbO and Bi2O3 on the radiation shielding and elastic features for different glasses. *J. Mater. Res. Technol.* **2020**, *9*, 8429–84381. [CrossRef]
23. Naseer, K.A.; Marimuthu, K.; Mahmoud, K.A.; Sayyed, M.I. The concentration impact of Yb3+ on the bismuth boro-phosphate glasses: Physical, structural, optical, elastic, and radiation-shielding properties. *Radiat. Phys. Chem.* **2021**, *188*, 109617. [CrossRef]
24. Hannachi, E.; Mahmoud, K.A.; Sayyed, M.I.; Slimani, Y. Effect of sintering conditions on the radiation shielding characteristics of YBCO superconducting ceramics. *J. Phys. Chem. Solids* **2022**, *164*, 110627. [CrossRef]
25. Sakar, E.; Özgür, F.; Bünyamin, A.; Sayyed, M.I.; Murat, K. Phy-X/PSD: Development of a user friendly online software for calculation of parameters relevant to radiation shielding and dosimetry. *Radiat. Phys. Chem.* **2020**, *166*, 108496. [CrossRef]